Human Movement Science 66 (2019) 133–141

Contents lists available at ScienceDirect

Human Movement Science

journal homepage: www.elsevier.com/locate/humov

Influence of fatigue on running coordination: A UCM analysis with a geometric 2D model and a subject-specific anthropometric 3D model

Felix Möhler*, Steffen Ringhof, Daniel Debertin, Thorsten Stein

BioMotion Center, Institute of Sports and Sports Science (IfSS), Karlsruhe Institute of Technology, Karlsruhe, Germany

ARTICLE INFO

Keywords:
Motor control
Variability
Synergy
Uncontrolled manifold
Locomotion

ABSTRACT

Although fatigue is a central issue in endurance sports little is known about the effects of fatigue on coordination. The uncontrolled manifold (UCM) approach has been widely used in recent studies to examine coordination in human movement; however, it has not been used to study the effects of fatigue on running. Therefore, the aim of this study was to analyze the effects of fatigue on the synergy structure stabilizing the center of mass (CoM) trajectory in experienced runners during high-intensity running using the UCM approach.

A total of 13 healthy young experienced runners participated in the study. Based on a lactate threshold testing undertaken one week prior to the measurements, participants were asked to run on a treadmill at their individual "fatigue-speed" until exhaustion. The kinematics of 20 consecutive gait cycles were recorded at the beginning (rested) and at the end (fatigue) of the protocol. The effects of fatigue on the synergy structure were investigated using a geometric 2D model and a subject-specific anthropometric 3D model. Specifically, the variance affecting the CoM trajectory ($UCM_{\perp}$), the variance not affecting the CoM trajectory ($UCM_{||}$), and their ratio (UCM_{Ratio}) were analyzed for different gait cycle phases (absorption, propulsion and flight phase).

Three-way repeated-measures ANOVA tests revealed differences between the two models. Fatigue-induced changes in the UCM structure could only be detected using the 3D model. UCM_{Ratio} did not change, but $UCM_{\perp}$ increased during flight phase. In the 2D model, UCM_{Ratio} and both components were higher during the propulsion phase than during the absorption phase in both the rested and the fatigued state.

Using a current concept for analyzing motor coordination, the UCM approach, only minor changes with fatigue were detected using the 3D subject-specific model. This indicates that the runners were able to control the trajectory of their CoM when fatigued. As the 2D model was not able to detect these changes, our study emphasizes that future studies on the effects of fatigue should focus on 3D analyses.

1. Introduction

Running is widely enjoyed as both a recreational and a competitive sport. To maintain running performance over a long distance, economy and resistance to fatigue are key factors (Hoogkamer, Kipp, Spiering, & Kram, 2016). Since it can be assumed that experienced runners have spent many years developing a running style that ensures economy, one might suppose that they will try to

* Corresponding author at: Engler-Bunte-Ring 15, 76131 Karlsruhe, Germany.
E-mail address: felix.moehler@kit.edu (F. Möhler).

https://doi.org/10.1016/j.humov.2019.03.016
Received 7 February 2019; Received in revised form 19 March 2019; Accepted 25 March 2019
Available online 11 April 2019
0167-9457/

maintain this running style in a fatigued state.

Studies on the effects of fatigue on running biomechanics have produced conflicting results (Winter, Gordon, & Watt, 2017). Most previous studies focused on spatiotemporal parameters or changes in isolated degrees of freedom (DoF) (Chan-Roper, Hunter, Myrer, Eggett, & Seeley, 2012; Maas, De Bie, Vanfleteren, Hoogkamer, & Vanwanseele, 2018; Strohrmann, Harms, Kappeler-Setz, & Tröster, 2012). In fatigued runners, Chan-Roper, Hunter, Myrer, Eggett, & Seeley (2012) found significant changes in knee flexion (decrease during support and increase during swing) and an increase in hip flexion and a decrease in hip extension (during swing). Maas et al. (2018) found an increased anterior pelvic tilt and increased pelvic rotation range of motion during stance phase as well as increased ankle plantar flexion during swing phase. Koblbauer, van Schooten, Verhagen, and van Dieën (2014) also found changes in trunk flexion-extension, which indicates that upper-body kinematics are also affected during fatigue. However, to gain a deeper understanding of the effects of fatigue on running coordination, approaches are needed that are based on models of motor control, to capture coordination in terms of the interplay of different degrees of freedom (Cowley & Gates, 2017). Against this background, there is a lack of research.

The framework of the uncontrolled manifold (UCM) hypothesis (Scholz & Schöner, 1999) is an established approach in the motor control literature for the analysis of motor coordination (Latash, Scholz, & Schöner, 2007). The fundamental hypothesis of the UCM approach is that elemental variables (EV) co-vary to stabilize a task-dependent performance variable (PV) (Scholz & Schöner, 1999). Thus, stabilization of the PV is reflected through a multitude of combinations of EVs across repetitions which lead to the same value of the PV. Hence, movement variability is split in two components: an orthogonal component ($UCM_{\perp}$), which changes the PV, and a parallel component ($UCM_{||}$), which does not (Latash et al., 2007; Scholz & Schöner, 1999). The parallel component is thought to stabilize the PV by representing flexible solutions for the movement task. The ratio of $UCM_{||}$ and $UCM_{\perp}$ (UCM_{Ratio}) is used as a measure of the degree of stability. Thus, if $UCM_{||}$ is greater than $UCM_{\perp}$, there is a “synergy” that stabilizes the PV (Latash, Scholz, & Schoner, 2002; Latash et al., 2007).

Within the UCM framework, some studies have assessed human walking (Black, Smith, Wu, & Ulrich, 2007; Krishnan, Rosenblatt, Latash, & Grabiner, 2013; Papi, Rowe, & Pomeroy, 2015; Qu, 2012; Robert, Bennett, Russell, Zirker, & Abel, 2009; Tawy, Rowe, & Biant, 2018; Vito, Tropea, Rinaldi, & Micera, 2018; Yen & Chang, 2010) and the effects of fatigue on walking (Qu, 2012). This last study showed that UCM_{Ratio} in the frontal plane decreased with fatigue, indicating that participants’ center of mass (CoM) trajectory was less stabilized when fatigued. In contrast to this result, research focusing on the effects of fatigue on movement coordination found changes in parts of the multi-element system, which compensated for the fatigue effects so that the stability of the movement outcome was not affected (Côté, Feldman, Mathieu, & Levin, 2008; Emery & Côté, 2012; Singh & Latash, 2011). This seems to be the case even in a finger force task with low redundancy (Singh, Zatsiorsky, & Latash, 2010). To date, however, no studies have analyzed the synergy-structure or the effects of fatigue on running.

Most previous studies that applied the UCM approach to analyze walking chose the body’s CoM as a PV (Black et al., 2007; Papi et al., 2015; Qu, 2012; Tawy et al., 2018; Vito et al., 2018) and joint angles as EV, except Black et al. (2007) who used segment angles. Others focused on the foot trajectory during swing phase (Krishnan et al., 2013; Rosenblatt, Latash, Hurt, & Grabiner, 2015). However, there are differences between these studies in the modelling of the CoM: they used either a purely geometrical model limited to one limb (Papi et al., 2015; Tawy et al., 2018; Vito et al., 2018) or a segmented-mass model (Black et al., 2007; Qu, 2012) to calculate the CoM. Since all of these models are restricted to two dimensions, Papi et al. (2015), pointed out the need for the development of a three dimensional model. The potential effects of models of different complexity on the outcome of UCM-analysis have not yet been investigated. Additionally, as stated above, fatigue leads to changes which do not exclusively take place in the sagittal plane or in the lower limbs (Maas et al., 2018; Qu, 2012). Thus, these effects might not be detectable by a simplified 2D-model.

Therefore, this study has two purposes: 1) to analyze the effects of fatigue on the synergy structure stabilizing the CoM trajectory during running and 2) to perform this analysis with two different models to better understand their influence on the outcome of the UCM analysis.

To this end, experienced runners were analyzed before and after a fatigue protocol using a UCM approach with two different models: a geometric 2D model developed by Papi et al. (2015) and a subject-specific anthropometric 3D model. We hypothesized that UCM_{Ratio} would decrease with increasing fatigue due to an increase of $UCM_{\perp}$. Since changes with fatigue do not exclusively happen in the sagittal plane, we hypothesized that the 3D model might detect these changes better than the geometric 2D model.

2. Methods

2.1. Participants

A total of 13 healthy young experienced male runners participated in the study (Table 1). The inclusion criteria were a 10 km record below 35 min (run within the last year); a minimum distance covered of 50 km/week during the eight weeks preceding the experiment and an active membership of a running club for at least two years. Exclusion criteria were recent injuries or pain in the lower limbs. All participants provided written informed consent. The study was approved by the ethics committee of the Karlsruhe Institute of Technology.

2.2. Experimental protocol

All participants came to the lab twice to perform two types of tests. The tests were conducted one week apart and at a similar time

Table 1
Sample characteristics (mean ± standard deviation); BMI = body mass index; VL3 = running speed at 3 mmol/L lactate.

Participants [n]	13
Age [years]	23.5 ± 3.6
Height [m]	1.80 ± 0.06
Weight [kg]	66.8 ± 5.4
BMI [kg/m^2]	20.6 ± 1.7
Physical activity (including running) [h/week]	8.2 ± 1.9
Running [h/week]	6.5 ± 1.7
Running training [years]	7.2 ± 3.2
10 km record [min:*sec*]	32:59 ± 01:19
VL3 [m/s]	4.67 ± 0.29

of the day on a treadmill (h/p/cosmos Saturn, Nussdorf-Traunstein, Germany) with a slope of 1% (Jones & Doust, 1996).

On day 1, participants performed a lactate threshold test. The test started at 8 km/h, the step duration was 3 min, the step increment was 2 km/h and the pause between the steps was 30 s. Blood lactate concentration was measured at the right ear prior to the test and after each step. Based on the lactate values and the critical power concept (Monod & Scherrer, 1965), an individual fatigue speed (FS) was determined. This speed was calculated as the speed that which participants should be able to run for a maximum of 10 min, and was used for the main measurement on day 2.

On day 2, the participants were first familiarized with the treadmill. The familiarization protocol consisted of 6 min of walking (Matsas, Taylor, & McBurney, 2000) followed by 6 min of running (Lavcanska, Taylor, & Schache, 2005). Afterwards, participants ran at their individual FS until exhaustion. Measurements were taken at two time points: the first one 15 s after the treadmill reached FS (considered the rested state), and the second one just before ultimate fatigue (considered the fatigued state). Participants were instructed to give notice about 20 s prior to exhaustion. In both states (rested, fatigued), 20 consecutive gait cycles were recorded.

Fatigue was confirmed using rating of perceived exertion on the Borg 15-grade scale (Borg, 1982). Participants were instructed to look ahead and to not perform undesired movements like looking at their wristwatch during their performance. To prevent falls, all participants were held in a safety harness during the experiment.

2.3. Data collection and processing

Prior to the measurements, 22 anthropometric measures were manually taken from each participant and 41 reflective markers were attached to participants' skin in accordance to the ALASKA modelling system (Advanced Lagrangian Solver in kinetic Analysis, insys GmbH, Chemnitz, Germany; (Härtel & Hermsdorf, 2006)). During the treadmill protocol, 11 Vicon MX cameras (Vicon Motion Systems; Oxford Metrics Group, Oxford, UK) were used to record the marker trajectories at 200 Hz. Afterwards, data were pre-processed using Vicon Nexus software V1.8.5 and filtered using a fourth order low-pass Butterworth filter with a cutoff-frequency of 10 Hz using MATLAB R2017b (The MathWorks, Natick, MA, USA). The recorded trajectories along with the anthropometric measures (22 measured manually, 43 determined from the reflective markers according to the requirements of the ALASKA modelling system) were used to determine joint angles through inverse kinematics calculations using the ALASKA-full-body Dynamicus model (Härtel & Hermsdorf, 2006). The 20 consecutive gait cycles were time-normalized (from right foot strike to right foot strike) to 100 time steps using custom-made MATLAB routines for each participant and condition. Foot strike was determined as the timeframe where the vertical speed of the heel or foot marker changed its sign and toe off was determined using vertical acceleration of the toe marker (Leitch, Stebbins, Paolini, & Zavatsky, 2011).

2.4. Uncontrolled manifold approach

In line with other studies, we chose the CoM as our PV and joint angles as our EVs (Black et al., 2007; Papi et al., 2015; Qu, 2012; Tawy et al., 2018; Vito et al., 2018). We chose two different models to calculate the CoM: a 2D geometric model (Papi et al., 2015; Tawy et al., 2018) and a subject-specific anthropometric 3D model. The 2D model approximated the CoM as a fixed point in the pelvis calculated along the leg. In the 3D model, the CoM was calculated as a weighted sum of the body segments. Each of these models provides the relationship between the EV (joint angles) and the PV (CoM). Building on this, we decomposed the variability into the proportion that affected the PV ($UCM_{\perp}$) and the proportion that did not affect the PV ($UCM_{||}$) (Latash et al., 2007; Scholz & Schöner, 1999).

2D geometric model

The 2D model is based on the model of Papi et al. (2015) and was restricted to the leg in the sagittal plane (Fig. 1, left). It consists of 4 segments and 4 degrees of freedom. The CoM is determined as the midpoint of the anterior and posterior superior iliac spines (Papi et al., 2015), which are indicated by the respective pelvis markers. The 2D position of the CoM $\boldsymbol{r}_{CoM\_2D}$ can be expressed using the angles between the foot and the ground (θ_G), at the ankle (θ_A), at the knee (θ_K) and at the hip (θ_H). The angles are defined as shown in Fig. 1, where A, K and H are the 2D positions of the ankle, knee and hip joint centers calculated by Dynamicus, C and M are

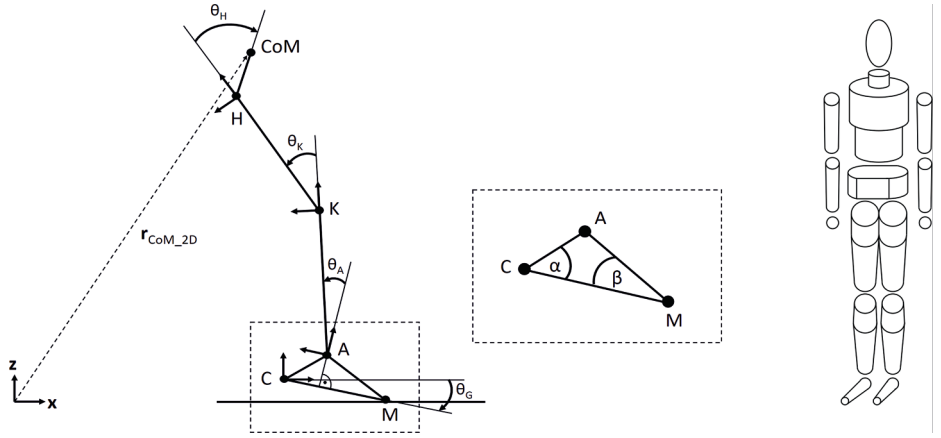

Fig. 1. Models for calculating CoM. Left: 2D geometric model; definition of the segment angles and positions used in the calculation of $\mathbf{r}_{CoM\_2D}$. Right: 3D anthropometric model.

the 2D positions of the heel and toe markers and α and β are the angles of the foot segment. A trigonometric analysis leads to:

$$r_{CoM\_2D} = \begin{pmatrix} x_A - AK\sin(\theta_G + \theta_A) - KH\sin(\theta_G + \theta_A + \theta_K) - HCoM\sin(\theta_G + \theta_A + \theta_K + \theta_H) \\ z_A + AK\cos(\theta_G + \theta_A) + KH\cos(\theta_G + \theta_A + \theta_K) + HCoM\cos(\theta_G + \theta_A + \theta_K + \theta_H) \end{pmatrix} \tag{1}$$

With

$$x_A = \begin{cases} x_C + CA\cos(\alpha + \theta_G) & z_M \geqslant z_C \\ x_M - MA\cos(\theta_G - \beta) & z_M < z_C \end{cases} \text{ and } z_A = \begin{cases} z_C + CA\sin(\alpha + \theta_G) & z_M \geqslant z_C \\ z_M - MA\sin(\theta_G - \beta) & z_M < z_C \end{cases} \tag{2}$$

This model can only be used in the stance phase and therefore the appropriate leg (left/right) was used during calculations for the relevant stance phase. The difference between the 3D segment length and the projected segment length was found to be marginal.

3D anthropometric model

The 3D model is based on Hanavan (1964) and consists of 17 segments and 50 degrees of freedom (47 segmental angles and 3 hip rotations, see Fig. 1, right). In addition to the Hanavan-model (Hanavan, 1964), we included a neck and a hip segment and modified some segments (e.g., the shape of the trunk was changed using more subject-specific measurements), leading to a total of 36 subject-specific anthropometric measurements (21 measured manually, 15 determined through the reflective markers). A constant density was assumed (Ackland, Henson, & Bailey, 1988). Each segment's mass was determined via volume integration.

Finally, the whole-body CoM ($\boldsymbol{r}_{CoM\_3D}$) was calculated as a weighted sum:

$$\boldsymbol{r}_{CoM\_3D} = \frac{1}{\sum_{i=1}^{N} V_i} * \sum_{i=1}^{N} \boldsymbol{r}_i V_i \tag{3}$$

With N as the number of segments; V_i as the volume of segment i; and $\boldsymbol{r}_i$ as the vector of the center of gravity of segment i.

UCM-based decomposition of stride-to-stride variability

Since we chose the CoM as a PV (Black et al., 2007; Papi et al., 2015), changes in joint angles (θ, EV's) were linked to changes in the CoM ($\boldsymbol{r}_{CoM}$, PV). Therefore, the PV is expressed as a function of the EV's: $PV = \boldsymbol{r}_{CoM} = f(EV) = f(\theta)$. Following the UCM approach (Black et al., 2007; Scholz & Schoener, 1999), the null space of the linearized Jacobian, representing the space in which alterations of the EV do not cause alterations of the PV, is calculated as:

$$0 = \boldsymbol{J}\boldsymbol{e}_i;\ \boldsymbol{J} = \left.\frac{\partial f(\theta)}{\partial \theta}\right|_{\theta_0};\ i = 1 \cdots n - d \tag{4}$$

θ_0 are the mean values of the EV over the 20 gait cycles, $\boldsymbol{e}_i$ are the vectors defining the null space, n is the number of dimensions of EV and d is the number of dimensions of the PV (here: $n = 4$ and $d = 2$ for the 2D model and $n = 50$ and $d = 3$ for the 3D model).

Deviations from the mean joint configuration (θ_0) were separated into those parallel to the UCM (those stabilizing the PV, $\sigma_{k,\parallel}$) and those orthogonal to the UCM (those changing the PV, $\sigma_{k,\perp}$). These calculations were performed for every percent of the gait cycle.

$$\sigma_{k,\parallel} = \sum_{i=1}^{n-d} [(\boldsymbol{e}_i^T(\theta_k - \theta_0))\boldsymbol{e}_i];\ \sigma_{k,\perp} = (\theta_k - \theta_0) - \sigma_{k,\parallel};\ k = 1 \cdots N_{cycle} \tag{5}$$

The variability parallel and orthogonal to the UCM was calculated as the variance over the $N_{cycle} = 20$ gait cycles:

$$UCM_{\parallel} = \sqrt{\frac{1}{(n-d) * N_{cycle}} \sum_{k=1}^{N_{cycle}} \sigma_{k,\parallel}^2} \tag{6a}$$

$$UCM_{\perp} = \sqrt{\frac{1}{d * N_{cycle}} \sum_{k=1}^{N_{cycle}} \sigma_{k,\perp}^2} \tag{6b}$$

The ratio between these two quantities was calculated as

$$UCM_{Ratio} = \frac{2 * UCM_{\parallel}2}{UCM_{\parallel}^2 + UCM_{\perp}2} - 1 \tag{7}$$

and quantifies the degree of stabilization of the CoM. This ratio lies between -1 and 1: a ratio > 0 is interpreted as a synergy, whereas a ratio ≤ 0 indicates no synergy (Papi et al., 2015; Tawy et al., 2018).

We divided the gait cycle in stance and flight phases. Following Novacheck (1998), stance was further divided in an absorption phase, characterized by a downward motion of the CoM, and a propulsion phase, characterized by an upwards motion of the CoM. For each of the phases we calculated the mean of each of the dependent variables (UCM_{Ratio}, $UCM_{\parallel}$ and $UCM_{\perp}$). For the 2D model, analyses could only be performed during stance.

2.5. Statistics

Statistical analyses were performed using JASP (http://www.jasp-stats.org). To test whether the control hypothesis about our PV ($UCM_{Ratio} > 0$) was fulfilled, one-sample t-tests were conducted.

To test if an influence of the choice of model exists, a $2 \times 2 \times 2$ ANOVA with factors state [rested, fatigued], model [2D, 3D] and phase [absorption, propulsion] was calculated for each dependent variable. Dependent t-tests (differences between gait cycle phases and states) were used as post-hoc tests. For the 3D model, a dependent *t*-test was used to look for differences between the rested and fatigued state for the flight phase.

The conditions for the application of ANOVA were tested a priori. Multiple t-tests are presented as corrected t-test's using the Holm-Bonferroni-correction (Holm, 1979). The significance level was set to $p = 0.05$. Partial eta square (η_p^2) and Cohen's d were used to indicate effect size for the ANOVA and t-tests, respectively. A small effect size was < 0.06 (η_p^2) or < 0.5 (Cohen's d). A moderate effect size was between 0.06 and 0.14 (η_p^2) or between 0.5 and 0.8 (Cohen's d). A large effect size was indicated by $\eta_p^2 > 0.14$ or Cohen's $d > 0.8$ (Cohen, 1992), respectively.

3. Results

FS calculated from the lactate threshold test on day 1 was at 19.27 ± 0.72 km/h. Participants were able to run at this speed for 4:06 ± 0:52 min and reported their perceived fatigue as 19.6 ± 0.65 on the Borg Scale (Borg, 1982).

The times courses of the UCM parameters are shown in Fig. 2. The mean values and standard deviations are listed in Table 2 and 3 for the 2D and 3D model, respectively. The three-way ANOVA showed no significant state effect or interactions involving the factor state for UCM_{Ratio} and $UCM_{\parallel}$. For $UCM_{\perp}$, the state effect showed a high effect size ($p = 0.110$, $\eta_p^2 = 0.199$). Significant model effects were detected for UCM_{Ratio} ($p < 0.001$, $\eta_p^2 = 0.627$) and $UCM_{\perp}$ ($p < 0.001$, $\eta_p^2 = 0.633$) as well as a high effect size for $UCM_{\parallel}$

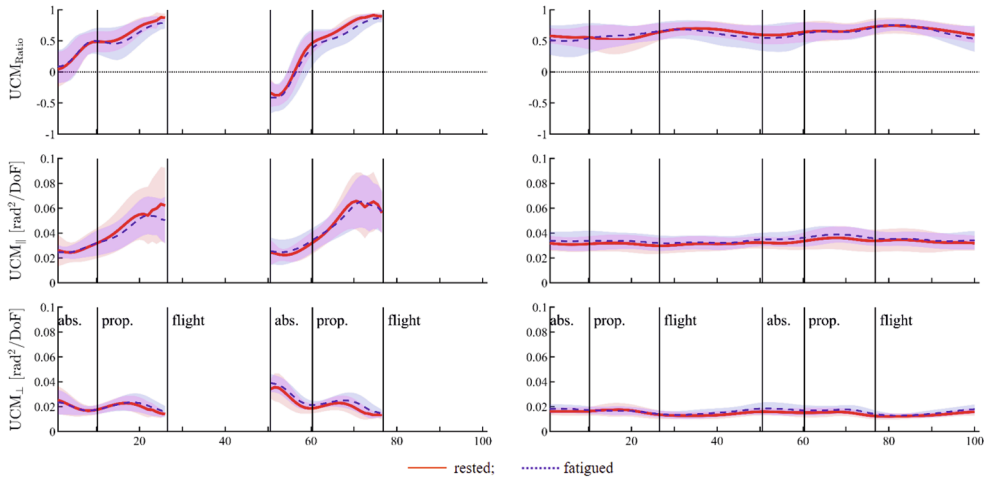

Fig. 2. Time courses for the three dependent UCM variables. Mean ± sd, for both models: 2D model (sagittal plane) to the left, and 3D model to the right. "abs." denotes the absorption phase, "prop." denotes the propulsion phase and "flight" denotes the flight phase.

Table 2
Mean ± sd for the three dependent variables, in the two stance phases (absorption, propulsion), calculated with the 2D geometric model.

		Rested	Fatigued
UCM_{Ratio}	Absorption	0.044 ± 0.174	0.063 ± 0.187
	Propulsion	0.664 ± 0.074	0.627 ± 0.103
	Flight		
$UCM_{\parallel}$	Absorption	0.026 ± 0.008	0.026 ± 0.006
	Propulsion	0.049 ± 0.016	0.049 ± 0.011
	Flight		
$UCM_{\perp}$	Absorption	0.024 ± 0.007	0.025 ± 0.005
	Propulsion	0.019 ± 0.005	0.021 ± 0.004
	Flight		

($p = 0.080$, $\eta_p^2 = 0.234$). For all three parameters, significant phase effects (all $p < 0.001$, $\eta_p^2 > 0.739$) and model × phase interactions were found (all $p < 0.001$, $\eta_p^2 > 694$). Since differences between the models occurred in all three dependent variables, the following results are presented separately for the 2D model and the 3D model.

3.1. Geometric 2D model

The post-hoc tests following the main effect for the factor state [rested, fatigued] for $UCM_{\perp}$ showed no influence of fatigue for neither absorption phase nor propulsion phase.

Concerning the phase effect [absorption, propulsion], dependent t-tests showed that UCM_{Ratio} significantly increased from absorption to propulsion phase in both the rested ($p < 0.001$, $d = 5.044$) and the fatigued ($p < 0.001$, $d = 3.113$) state.

Moreover, the UCM_{Ratio} was significantly above zero for both phases of the rested state (absorption: $p = 0.043$, $d = 0.627$; propulsion: $p < 0.001$, $d = 8.937$) and for the propulsion phase but not the absorption phase ($p = 0.245$, $d = 0.339$) of the fatigued state ($p < 0.001$, $d = 6.098$).

For $UCM_{\parallel}$, post hoc tests showed that in both the rested and the fatigued state, $UCM_{\parallel}$ increased from absorption to propulsion (rested: $p < 0.001$, $d = 2.526$; fatigued: $p < 0.001$, $d = 2.067$).

For $UCM_{\perp}$, post-hoc tests showed a decrease from absorption phase to propulsion phase in both the rested and the fatigued state (rested: $p < 0.001$, $d = 1.370$; fatigued: $p = 0.001$, $d = 1.269$).

3.2. Anthropometric 3D model

Post-hoc tests following the main effect for the factor state [rested, fatigued] for $UCM_{\perp}$ in the $2 \times 2 \times 2$ ANOVA showed no influence of fatigue showed now significant results. The dependent t-tests for the flight phase showed a significant increase with fatigue, with a medium effect size ($p = 0.041$, $d = 0.635$).

Concerning the post-hoc tests for the phase effect [absorption, propulsion] for UCM_{Ratio}, there were no significant differences. One-sample t-tests showed that UCM_{Ratio} was significantly above zero throughout the gait cycle in both the rested and the fatigued states ($p < 0.001$ in all cases, $d \geq 2.542$). For $UCM_{\parallel}$, the post-hoc tests showed a significant increase with a medium effect size from absorption to propulsion phase in both the rested ($p = 0.032$, $d = 0.671$) and the fatigued ($p = 0.020$, $d = 0.742$) state. For $UCM_{\perp}$ there were no significant effects.

Table 3
Mean ± sd values for the three dependent variables, in the three phases (absorption, propulsion, flight), calculated with the 3D anthropometric model.

		Rested	Fatigued
UCM_{Ratio}	Absorption	0.582 ± 0.132	0.536 ± 0.211
	Propulsion	0.600 ± 0.160	0.615 ± 0.137
	Flight	0.679 ± 0.102	0.652 ± 0.127
$UCM_{\parallel}$	Absorption	0.032 ± 0.005	0.034 ± 0.006
	Propulsion	0.033 ± 0.007	0.036 ± 0.006
	Flight	0.032 ± 0.006	0.033 ± 0.005
$UCM_{\perp}$	Absorption	0.016 ± 0.003	0.018 ± 0.004
	Propulsion	0.016 ± 0.004	0.017 ± 0.003
	Flight	0.013 ± 0.002	0.015 ± 0.003

4. Discussion

This is the first study to analyze the effects of fatigue during running within the framework of the UCM hypothesis in experienced runners. We analyzed the synergy stabilizing the CoM trajectory in both a rested and a fatigued state. Neither of the two models detected fatigue effects for the UCM_{Ratio}. Therefore, our first hypothesis, stating that UCM_{Ratio} would decrease with increasing fatigue, had to be renounced. Our second hypothesis was partly confirmed: The 3D anthropometric model found a significant effect of the fatigue protocol in $UCM_{\perp}$ in the flight phase. Since the two models showed different results, the effects of fatigue are discussed for each model separately.

4.1. Fatigue effects

All participants were considerably fatigued as indicated by their rating on the Borg scale (19.6 ± 0.65).

The 2D model showed an increasing UCM_{Ratio} throughout the stance phase. During the absorption phase, UCM_{Ratio} was not significantly different from zero in the fatigued state. In the propulsion phase for both the rested and the fatigued state and in the absorption phase for the rested state, UCM_{Ratio} was significantly above zero. This means that, during the absorption phase for the fatigued state, there was no synergy stabilizing the CoM trajectory. This is also reflected in the two variability components. $UCM_{||}$, which stabilizes the PV by offering flexible solutions (Latash, Scholz, Schoner, 2002), was higher during the propulsion phase than during the absorption phase. In contrast, $UCM_{\perp}$, which changes the PV and is thus potentially detrimental for performance, was lower during propulsion compared to absorption. So the geometric 2D model implies that exhausted runners were no longer able to stabilize their CoM trajectory during the absorption phase, although this development did not reach significance. In addition, it has to be kept in mind that the 2D model is restricted to the sagittal plane and does not take into account any parts of the upper body which are also affected by running-induced fatigue (Koblbauer et al., 2014).

Within the 3D model, UCM_{Ratio} was always above zero, indicating that there was a synergy present over the whole gait cycle. For UCM_{Ratio} and $UCM_{\perp}$, there was no difference throughout stance for either the rested or fatigued state. $UCM_{||}$ increased from absorption to propulsion, but to a smaller degree than in the 2D model. For both UCM_{Ratio} and $UCM_{||}$, there were no effects with fatigue. $UCM_{\perp}$ increased with fatigue during the flight phase. Since $UCM_{\perp}$ represents variability influencing the PV (Latash, ML, Scholz, JP, Schoner, 2002), it has to be avoided to reach a constant performance from stride-to-stride. The increase with fatigue might show that runners cannot maintain their stride-to-stride consistency in a fatigued state. The trajectory of the CoM during flight is largely determined at toe-off: alterations during flight are a result of alterations during toe-off. Since there were no fatigue effects detected during the propulsion phase, these might develop during the course of the flight phase. Since this effect only showed a medium effect size, it is questionable whether it is significant in practice.

Previous studies on the effects of fatigue on movement coordination frequently found an increase in $UCM_{||}$, indicating that variability increased without affecting the movement outcome (Côté et al., 2008; Emery & Côté, 2012; Singh & Latash, 2011). Common to these studies was that the fatigue protocol concerned one element of the multi-element system. The non-affected elements of the system seemed to compensate for this impairment. Similar to the fatigue protocol applied by Qu (2012), our fatigue protocol intended to induce a “whole-body-fatigue”. So there were no non-affected elements which could account for the fatigue-effects. This might explain the decreased UCM_{Ratio} in the frontal plane in the study by Qu (2012). In contrast to Qu (2012), our study focused on running experts. Running experts are used to running in a fatigued state in training and competition. Accordingly, the athletes in our study are used to maintaining their running style in a fatigued state. Hoenig, Hamacher, Braumann, Zech, and Hollander (2018) studied the local dynamic stability during a 5000 m run in recreational and competitive runners and found an increase with fatigue in both groups. However, since the same kinematic pattern can be generated by different muscle activations due to the redundancy of the musculoskeletal system, it is possible that the effects of fatigue could be detectable at the muscle level (Hollman, Hohl, Kraft, Strauss, & Traver, 2012). Compensation strategies on a muscular level as observed by Singh and Latash (2011) or Nielsen et al. (2018) might also be of importance in our study. Therefore, it might be promising to study fatigue effects in running within the UCM framework using modules calculated from EMG data as EVs, like it wasdone before in a postural control task (Krishnamoorthy, Latash, Scholz, & Zatsiorsky, 2003; Singh & Latash, 2011).

The fact that no fatigue effects were found in this study does not necessarily mean that they are not present in the studied kinematics. It could be speculated that runners adopted a different locomotion pattern in the fatigued state. Since the CoM is an important performance variable, it remains closely controlled and therefore changes are not detectable with the UCM approach. The use of a matrix factorization technique such as principal component analysis (Cowley & Gates, 2017; Daffertshofer, Lamoth, Meijer, & Beek, 2004) could help to detect such changes in kinematics while taking into account the interplay of the different DoFs.

4.2. Modeling

We assumed the CoM to be a good choice of a performance variable in running (Black et al., 2007; Papi et al., 2015), since the running human body has been successfully modelled as a spring-mass model (Blickhan, 1989; Dutto & Smith, 2002). It has been shown that runners adjust their running speed rather than the vertical position of their CoM, so CoM-control seems to have a high priority (Girard, Millet, Slawinski, Racinais, & Jean-Paul, 2013). Our finding, that the control of the CoM is not impaired by fatigue, supports this assumption. In the UCM literature, two different approaches have been employed to link changes in the EVs with changes in the PV. One can either build up a multi-body model or use a multiple linear regression technique, both techniques have been shown to produce equivalent results (Freitas, Scholz, & Latash, 2010; Freitas & Scholz, 2010). We chose an approach using a

multi-body model.

As stated earlier, fatigue effects are observed in all three planes, in the lower and upper body and during stance and flight phase (Chan-Roper et al., 2012; Koblbauer et al., 2014; Maas et al., 2018). We therefore developed a 3D anthropometric whole-body model. Since athletes are a special anthropometric group (Virmavirta & Isolehto, 2014), the use of a subject-specific model seemed appropriate. We performed our analysis with this model and with a literature-based 2D model (Papi et al., 2015). Since there is no fixed support during flight phase, the geometric 2D model could only be used during stance. Because of that, an anthropometric 3D model should be used to study the effects of fatigue on running gait.

4.3. Limitations

To capture the natural variability over several repetitions of the same movement, consecutive gait cycles were captured and measurements were therefore performed on a treadmill. However, running on a treadmill is not identical to running overground (Fellin, Davis, & Manal, 2012). Since participants were given sufficient time for familiarization with the treadmill (Lavcanska et al., 2005; Matsas et al., 2000), it can be assumed that movement patterns were at least stable, if not identical to ones from overground running (Riley et al., 2008). The choice of the PV in the UCM framework is a subjective one. Different PVs have been used in studies dealing with human locomotion (Krishnan et al., 2013; Robert et al., 2009). There might not be one correct choice, but instead several important variables. However, as the CoM trajectory is highly controlled even in the fatigued state, CoM trajectory control seems to be a high priority for the central nervous system and thus is a reasonable choice.

5. Conclusions

The understanding of fatigue effects on running coordination is an important issue in sport science. Studies analyzing the effects of fatigue on running using discrete kinematic parameters show only limited evidence concerning the effects of fatigue (Winter et al., 2017). Applying current concepts from motor control to the field of sport science is a promising direction to gain deeper insights. The effects of fatigue might be better addressed at the level of motor coordination while taking into account the interplay of different DoFs (Sternad, 2018). Using a current concept for motor coordination, the UCM approach, minor changes with fatigue could be detected using a 3D subject-specific model: the orthogonal component increased during flight phase, without affecting the UCM_{Ratio}. Runners thus seem to be able to control the trajectory of their CoM under fatigue.

Declaration of interest

All authors disclose any financial and personal relationships with other people or organizations that could inappropriately influence this work.

Acknowledgements

The authors would like to thank Frieder Krafft and Gunther Kurz for helping out by conducting the lactate threshold testing. The authors also would like to thank Sonja Marahrens for her help in setting up the model.

This research did not receive any specific grant from funding agencies in the public, commercial, or not-for-profit sectors.

Appendix A. Supplementary data

Supplementary data to this article can be found online at https://doi.org/10.1016/j.humov.2019.03.016.

References

Ackland, T. R., Henson, P. W., & Bailey, D. A. (1988). The uniform density assumption: its effect upon the estimation of body segment inertial parameters. *International Journal of Sport Biomechanics, 4*(2), 146–155. https://doi.org/10.1123/ijsb.4.2.146.

Black, D. P., Smith, B. A., Wu, J., & Ulrich, B. D. (2007). Uncontrolled manifold analysis of segmental angle variability during walking: Preadolescents with and without Down syndrome. *Experimental Brain Research, 183*(4), 511–521. https://doi.org/10.1007/s00221-007-1066-1.

Blickhan, R. (1989). The spring-mass model for running and hopping. *Journal of Biomechanics, 22*(11), 1217–1227. https://doi.org/https://doi.org/10.1016/0021-9290(89)90224-8.

Borg, G. A. (1982). Psychophysical bases of perceived exertion. *Medicine and Science in Sports and Exercise, 14*, 377–381.

Chan-Roper, M., Hunter, I., W Myrer, J., L Eggett, D., & K Seeley, M. (2012). Kinematic changes during a marathon for fast and slow runners. *Journal of Sports Science & Medicine, 11*(1), 77–82.

Cohen, J. (1992). A power primer. *Psychological Bulletin, 112*(1), 155–159. https://doi.org/10.1037/0033-2909.112.1.155.

Côté, J. N., Feldman, A. G., Mathieu, P. A., & Levin, M. F. (2008). Effects of fatigue on intermuscular coordination during repetitive hammering. *Motor Control, 12*(2), 79–92. https://doi.org/10.1123/mcj.12.2.79.

Cowley, J. C., & Gates, D. H. (2017). Inter-joint coordination changes during and after muscle fatigue. *Human Movement Science, 56*, 109–118. https://doi.org/https://doi.org/10.1016/j.humov.2017.10.015.

Daffertshofer, A., Lamoth, C. J. C., Meijer, O. G., & Beek, P. J. (2004). PCA in studying coordination and variability: A tutorial. *Clinical Biomechanics, 19*(4), 415–428. https://doi.org/10.1016/j.clinbiomech.2004.01.005.

Dutto, D. J., & Smith, G. A. (2002). Changes in spring-mass characteristics during treadmill running to exhaustion. *Medicine & Science in Sports & Exercise, 34*(8), 1324–1331. https://doi.org/10.1097/00005768-200208000-00014.

Emery, K., & Côté, J. N. (2012). Repetitive arm motion-induced fatigue affects shoulder but not endpoint position sense. *Experimental Brain Research, 216*(4), 553–564.

https://doi.org/10.1007/s00221-011-2959-6.
Fellin, R. E., Davis, I. S., & Manal, K. (2012). Comparison of lower extremity kinematic curves during overground and treadmill running. *Journal of Applied Biomechanics, 26*(4), 407–414. https://doi.org/10.1123/jab.26.4.407.
Freitas, S. M. S. F., & Scholz, J. P. (2010). A comparison of methods for identifying the Jacobian for uncontrolled manifold variance analysis. *Journal of Biomechanics, 43*(4), 775–777. https://doi.org/10.1016/j.jbiomech.2009.10.033.
Freitas, S. M. S. F., Scholz, J. P., & Latash, M. L. (2010). Analyses of joint variance related to voluntary whole-body movements performed in standing. *Journal of Neuroscience Methods, 188*(1), 89–96. https://doi.org/10.1016/j.jneumeth.2010.01.023.
Girard, O., Millet, G., Slawinski, J., Racinais, S., & Jean-Paul, M. (2013). Changes in running mechanics and spring-mass behaviour during a 5-km time trial. *International Journal of Sports Medicine, 34*(9), 832–840. https://doi.org/10.1055/s-0032-1329958.
Hanavan, E. P. J. (1964). A mathematical model of the human body. (AMRL-TR-64). Ohio, United States: Aerospace Medical Research Laboratories.
Härtel, T., & Hermsdorf, H. (2006). Biomechanical modelling and simulation of human body by means of DYNAMICUS. *Journal of Biomechanics, 39*, 549. https://doi.org/10.1016/S0021-9290(06)85262-0.
Hoenig, T., Hamacher, D., Braumann, K.-M., Zech, A., & Hollander, K. (2018). Analysis of running stability during 5000 m running. *European Journal of Sport Science, 1–9*. https://doi.org/10.1080/17461391.2018.1519040.
Hollman, J. H., Hohl, J. M., Kraft, J. L., Strauss, J. D., & Traver, K. J. (2012). Effects of hip extensor fatigue on lower extremity kinematics during a jump-landing task in women: A controlled laboratory study. *Clinical Biomechanics, 27*(9), 903–909. https://doi.org/https://doi.org/10.1016/j.clinbiomech.2012.07.004.
Holm, S. (1979). A simple sequentially rejective multiple test procedure. *Scandinavian Journal of Statistics, 6*(2), 65–70. https://doi.org/10.2307/4615733.
Hoogkamer, W., Kipp, S., Spiering, B. A., & Kram, R. (2016). Altered running economy directly translates to altered distance-running performance. *Medicine and Science in Sports and Exercise, 48*, 2175–2180. https://doi.org/10.1249/MSS.0000000000001012.
Jones, A. M., & Doust, J. H. (1996). A 1% treadmill grade most accurately reflects the energetic cost of outdoor running. *Journal of Sports Sciences, 14*(4), 321–327. https://doi.org/10.1080/02640419608727717.
Koblbauer, I. F., van Schooten, K. S., Verhagen, E. A., & van Dieën, J. H. (2014). Kinematic changes during running-induced fatigue and relations with core endurance in novice runners. *Journal of Science and Medicine in Sport, 17*(4), 419–424. https://doi.org/10.1016/j.jsams.2013.05.013.
Krishnamoorthy, V., Latash, M. L., Scholz, J. P., & Zatsiorsky, V. M. (2003). Muscle synergies during shifts of the center of pressure by standing persons. *Experimental Brain Research, 152*(3), 281–292. https://doi.org/10.1007/s00221-003-1574-6.
Krishnan, V., Rosenblatt, N. J., Latash, M. L., & Grabiner, M. D. (2013). The effects of age on stabilization of the mediolateral trajectory of the swing foot. *Gait and Posture, 38*(4), 923–928. https://doi.org/10.1016/j.gaitpost.2013.04.023.
Latash, M. L., Scholz, J. P., … Schoner, G. (2002). Motor control strategies revealed in the structure of motor… : Exercise and sport sciences reviews. *Exercise and Sport Sciences Reviews, 30*(1), 26–31. https://doi.org/10.1097/00003677-200201000-00006.
Latash, M., Scholz, J., & Schöner, G. (2007). Toward a new theory of motor synergies. *Motor Control, 11*(3), 276–308. https://doi.org/10.1123/mcj.11.3.276.
Lavcanska, V., Taylor, N. F., & Schache, A. G. (2005). Familiarization to treadmill running in young unimpaired adults. *Human Movement Science, 24*(4), 544–557. https://doi.org/10.1016/j.humov.2005.08.001.
Leitch, J., Stebbins, J., Paolini, G., & Zavatsky, A. B. (2011). Identifying gait events without a force plate during running: A comparison of methods. *Gait and Posture, 33*(1), 130–132. https://doi.org/10.1016/j.gaitpost.2010.06.009.
Maas, E., De Bie, J., Vanfleteren, R., Hoogkamer, W., & Vanwanseele, B. (2018). Novice runners show greater changes in kinematics with fatigue compared with competitive runners. *Sports Biomechanics, 17*(3), 350–360. https://doi.org/10.1080/14763141.2017.1347193.
Matsas, A., Taylor, N., & McBurney, H. (2000). Knee joint kinematics from familiarised treadmill walking can be generalised to overground walking in young unimpaired subjects. *Gait and Posture, 11*(1), 46–53. https://doi.org/10.1016/S0966-6362(99)00048-X.
Monod, H., & Scherrer, J. (1965). The work capacity of a synergic muscular group. *Ergonomics, 8*(3), 329–338. https://doi.org/10.1080/00140136508930810.
Nielsen, N.-P., Hug, F., Guével, A., Colloud, F., Lardy, J., & Dorel, S. (2018). Changes in motor coordination induced by local fatigue during a sprint cycling task. *Medicine & Science in Sports & Exercise, 50*, 1394–1404. https://doi.org/10.1249/MSS.0000000000001572.
Novacheck, T. F. (1998). The biomechanics of running. *Gait & Posture, 7*(1), 77–95. https://doi.org/https://doi.org/10.1016/S0966-6362(97)00038-6.
Papi, E., Rowe, P. J., & Pomeroy, V. M. (2015). Analysis of gait within the uncontrolled manifold hypothesis: Stabilisation of the centre of mass during gait. *Journal of Biomechanics, 48*(2), 324–331. https://doi.org/10.1016/j.jbiomech.2014.11.024.
Qu, X. (2012). Uncontrolled manifold analysis of gait variability: Effects of load carriage and fatigue. *Gait and Posture, 36*(2), 325–329. https://doi.org/10.1016/j.gaitpost.2012.03.004.
Riley, P., Dicharry, J., Franz, J., Della Croce, U., P Wilde, R., & Kerrigan, D. (2008). A kinematics and kinetic comparison of overground and treadmill running. *Medicine and Science in Sports and Exercise, 40*(6), 1093–1100. https://doi.org/10.1249/MSS.0b013e3181677530.
Robert, T., Bennett, B. C., Russell, S. D., Zirker, C. A., & Abel, M. F. (2009). Angular momentum synergies during walking. *Experimental Brain Research, 197*(2), 185–197. https://doi.org/10.1007/s00221-009-1904-4.
Rosenblatt, N. J., Latash, M. L., Hurt, C. P., & Grabiner, M. D. (2015). Challenging gait leads to stronger lower-limb kinematic synergies: The effects of walking within a more narrow pathway. *Neuroscience Letters, 600*, 110–114. https://doi.org/10.1016/J.NEULET.2015.05.039.
Scholz, J. P., & Schoener, G. (1999). The uncontrolled manifold concept: Identifying control variables for a functional task. *Experimental Brain Research, 126*(3), 289–306. https://doi.org/10.1007/s002210050738.
Scholz, J. P., & Schöner, G. (1999). The uncontrolled manifold concept: Identifying control variables for a functional task. *Experimental Brain Research, 126*(3), 289–306. https://doi.org/10.1007/s002210050738.
Singh, T., & Latash, M. L. (2011). Effects of muscle fatigue on multi-muscle synergies. *Experimental Brain Research, 214*(3), 335–350. https://doi.org/10.1007/s00221-011-2831-8.
Singh, T., Varadhan, S. K., Zatsiorsky, V. M., & Latash, M. L. (2010). Fatigue and motor redundancy: adaptive increase in finger force variance in multi-finger tasks. *Journal of Neurophysiology, 103*(6), 2990–3000. https://doi.org/10.1152/jn.00077.2010.
Sternad, D. (2018). It's not (only) the mean that matters: Variability, noise and exploration in skill learning. *Current Opinion in Behavioral Sciences, 20*, 183–195. https://doi.org/https://doi.org/10.1016/j.cobeha.2018.01.004.
Strohrmann, C., Harms, H., Kappeler-Setz, C., & Tröster, G. (2012). Monitoring kinematic changes with fatigue in running using body-worn sensors. *IEEE Transactions on Information Technology in Biomedicine, 16*(5), 983–990. https://doi.org/10.1109/TITB.2012.2201950.
Tawy, G. F., Rowe, P., & Biant, L. (2018). Gait variability and motor control in patients with knee osteoarthritis as measured by the uncontrolled manifold technique. *Gait and Posture, 59*, 272–277. https://doi.org/10.1016/j.gaitpost.2017.08.015.
Virmavirta, M., & Isolehto, J. (2014). Determining the location of the body's center of mass for different groups of physically active people. *Journal of Biomechanics, 47*(8), 1909–1913. https://doi.org/10.1016/j.jbiomech.2014.04.001.
Vito, M., Tropea, P., Rinaldi, L. A., & Micera, S. (2018). Uncontrolled manifold hypothesis: Organization of leg joint variance in humans while walking in a wide range of speeds. *Human Movement Science, 57*, 227–235. https://doi.org/10.1016/J.HUMOV.2017.08.019.
Winter, S., Gordon, S., & Watt, K. (2017). Effects of fatigue on kinematics and kinetics during overground running: A systematic review. *The Journal of Sports Medicine and Physical Fitness, 57*(6), 887–899. https://doi.org/10.23736/s0022-4707.16.06339-8.
Yen, J. T., & Chang, Y.-H. (2010). Rate-dependent control strategies stabilize limb forces during human locomotion. *Journal of The Royal Society Interface, 7*(46), 801–810. https://doi.org/10.1098/rsif.2009.0296.